Chapter 1

Introduction

1.1 The Relativistic Heavy Ion Collider, RHIC

RHIC consists of two six-fold symmetric superconducting rings with a circumference of 3.833 km. The two rings (blue and yellow) consist of six arcs intersecting at six interaction regions (IRs) and provide collisions to 2-4 concurrent experiments. The main goal of RHIC is to provide collisions at energies up to 100 GeV/u per beam for heavy ions ($^{197}Au^{79}$). The accelerator is also designed for colliding lighter ions all the way down to protons (250 GeV), including polarized protons [1, 2]. RHIC currently offers a unique feature to collide different ion species, for example deuteron-gold collisions in 2002. A sketch of the BNL accelerator complex, showing the RHIC injectors, beamlines, and location of the interaction regions is shown in Fig 1.1.

An important figure of merit for colliders is luminosity which defines the number of interactions produced per unit cross section given by the convolution integral [3]

$$\mathcal{L} = \int_A N_1 \rho_1(x,y) N_2 \rho_2(x,y)\ da \tag{1.1}$$

where $N_{1,2}$ are the number of particles per beam, and $\rho_{1,2}(x,y)$ are the transverse particle distributions [1]. For Gaussian beams with equal beam sizes, Eq. 1.1 becomes [5]

$$\mathcal{L} = n\frac{f_{rev} N_1 N_2}{4\pi\sigma_x^*\sigma_y^*} \tag{1.2}$$

where n is the number of bunches, f_{rev} is the revolution frequency, and $\sigma_{x,y}^*$ are the RMS widths of the Gaussian beam. For experiments the integrated

[1] Note that this integral holds for head on collision and short bunches. For bunches with $\sigma_z < \beta^*$, a luminosity reduction due to hourglass effect [4] is non-negligible like in p-p collisions at RHIC.

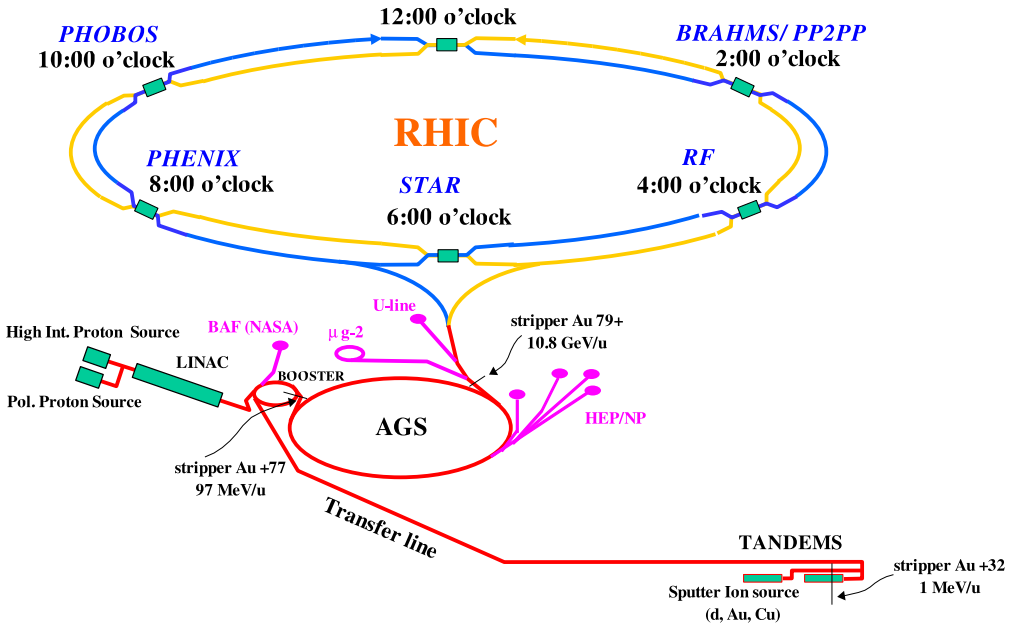

Figure 1.1: The hadron collider complex at Brookhaven National Laboratory. The path of a Au ion can be traced from its creation at the Tandem until its injection into RHIC. The polarized protons are injected from the LINAC into the booster ring, AGS, and finally into RHIC.

luminosity is a better figure of merit than the instantaneous luminosity given in Eq. 1.2. RHIC was commissioned in 1999 and has successfully completed five physics runs with heavy-ions and polarized protons. Table 1.1 shows design, achieved, and upgrade machine parameters. Fig. 1.2 shows an evolution of the nucleon-pair luminosity (A_1A_2L) indicative of the length of the runs as delivered to the PHENIX experiment.

Future luminosity upgrades involve electron cooling of the ion beams which is discussed in Part II of this thesis.

1.2 Linear Beam Dynamics

In a circular accelerator, the motion of a particle can be expressed as oscillations around a momentum dependent closed orbit [2] commonly know as

[2]The average particle trajectory closes on itself after one complete revolution

Table 1.1: Ion performance evolution and Run-# parameters shown for the RHIC collider. Note that some runs have collisions with different energies and the integrated luminosity listed is summed up over the different modes. The flexibility of different collision energies is an important aspect of RHIC. Enhanced luminosity numbers are facility goals c. 2008, before electron cooling [18].

Run	Species	No of bunches	Ions/bunch [10^9]	$\beta^\star$ [m]	Emittance [$\pi\mu$rad]	$\mathcal{L}_{int}$
Design	Au-Au	56	1.0	2	-	-
Run-1	Au-Au	56	0.5	3	15	20 μb^{-1}
Run-2	Au-Au	55	0.6	1-3	15-40	258.4 μb^{-1}
	p-p	55	70	3	25	1.4 pb^{-1}
Run-3	d-Au	55/110	120d/0.7Au	2	15-25	73 nb^{-1}
	p-p	55	70	1	20	5.5 pb^{-}1
Run-4	Au-Au	45	1.1	1-3	15-40	3.80 nb^{-1}
	p-p	56	70	1	20	7.1 pb^{-1}
Run-5	Cu-Cu	35-56	3.1-4.5	0.85-3	15-30	43.6 nb^{-1}
	p-p	56-106	60-90	1-2	25-50	29.6 pb^{-1}
Enhanced	Au-Au	112	1.1	0.9	15-40	-
Enhanced	p-p	112	2.0	1	25-50	-

betatron motion. The transverse motion can be expressed as

$$x(s) = x_0(s) + x_\beta(s) + D_x(s)\delta \tag{1.3}$$

where, $x_0(s)$ is the reference closed orbit, x_β is the betatron amplitude, and $\delta \equiv \Delta p/p_0$ is the momentum deviation from the ideal particle with momentum p_0 and D_x is the dispersion function.

1.2.1 Transverse Betatron Motion

Assuming no dispersion and small amplitude betatron oscillation around the closed orbit, the motion of the particles are governed by second order homogeous differential equations also know as Hill's equations

$$x^{''} + K_x(s)x(s) = 0 \tag{1.4}$$
$$y^{''} + K_y(s)y(s) = 0 \tag{1.5}$$

where,

$$K_x \equiv \frac{1}{\rho^2} - \frac{\partial B_y}{\partial x}\frac{1}{B\rho}, \quad K_y \equiv \frac{\partial B_y}{\partial x}\frac{1}{B\rho}$$

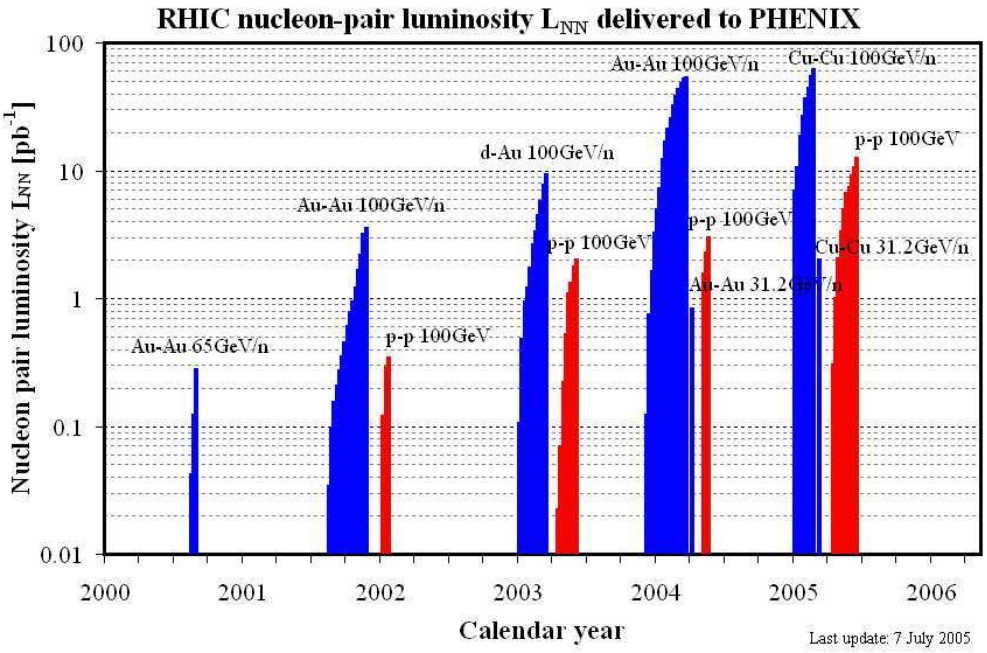

Figure 1.2: Nucleon-pair luminosity A_1A_2L delivered to the PHENIX experiment (courtesy RHIC operations).

The solution to the 2^{nd} order differential equations are

$$x(s) = \sqrt{2J\beta(s)}\cos\left(\psi(s)+\phi\right) \tag{1.6}$$

$$x'(s) = \sqrt{\frac{2J}{\beta(s)}}\left[\sin\left(\psi(s)+\phi\right)+\alpha(s)\cos\left(\psi(s)+\phi\right)\right] \tag{1.7}$$

where J and ϕ are action angle invariants of motion, $\beta(s)$ is the betatron function, $\alpha(s) \equiv -\beta'(s)/2$, and $\psi(s)$ is the phase advance given by

$$\psi(s_1 \rightarrow s_2) = \int_{s_1}^{s_2} \frac{1}{\beta(s)}\, ds \tag{1.8}$$

Assuming that the motion of the particle is linear motion, the evolution of the transverse coordinates of the particle motion in one turn can be conveniently expressed through a linear matrix

$$\begin{bmatrix} x \\ x' \end{bmatrix}_2 = \mathcal{M}_C \begin{bmatrix} x \\ x' \end{bmatrix}_1 \tag{1.9}$$

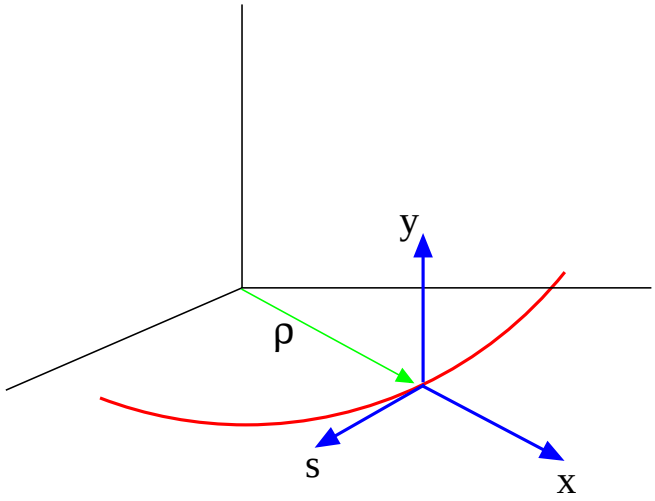

Figure 1.3: Frenet-Serret (curvilinear) coordinate system to describe particle motion in an accelerator.

where C is the circumference of the accelerator and

$$\mathcal{M}_C = \mathbf{I}\cos(\psi_C) + \mathbf{J}\sin(\psi_C). \tag{1.10}$$

Here, $\mathbf{I}$ is the 2×2 identity matrix, and

$$\mathbf{J} = \begin{bmatrix} \alpha & \beta \\ -\gamma & -\alpha \end{bmatrix} \tag{1.11}$$

where $\gamma \equiv (1+\alpha^2)/\beta$ and stable motion of the particle requires

$$|tr\mathcal{M}_C| \leq 2. \tag{1.12}$$

1.2.2 Emittance

The action variable J can be expressed in terms of x and x' to yield the Courant-Snyder invariant given by [22]

$$2J = \gamma x^2 + 2\alpha x x' + \beta x'^2 = \epsilon \tag{1.13}$$

The trajectory of the particle in the (x, x') frame follows an ellipse with an area of $2\pi J$ as shown in Fig. 1.4. When particles are subject to acceleration, it is useful to define a normalized emittance

$$\epsilon_N = \beta_r \gamma_r \epsilon \tag{1.14}$$

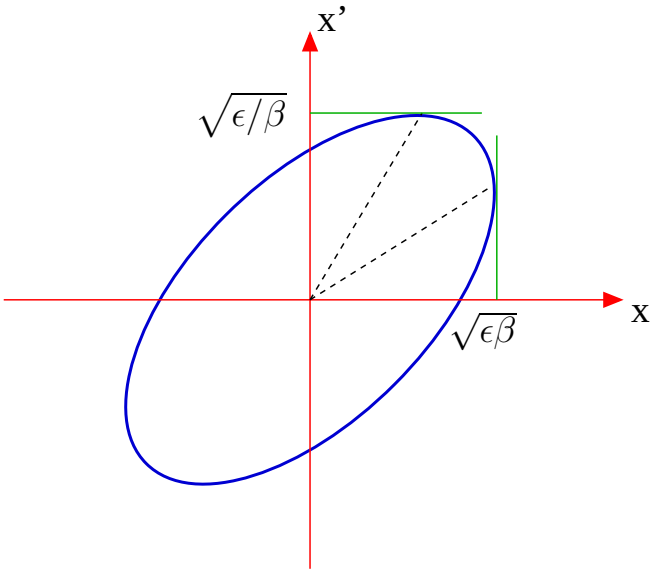

Figure 1.4: The Courant-Snyder invariant ellipse with an area of $\pi\epsilon$.

which is generally conserved. Here, β_r and γ_r are relativistic factors.

Given a distribution of particles, each tracing an ellipse, the rms beam emittance can be defined as [7]

$$\epsilon_{rms} = \sqrt{\sigma_x^2 \sigma_{x'}^2 - \sigma_{xx'}^2} \tag{1.15}$$

where

$$\sigma_x^2 = \int [x - \langle x \rangle]^2 \ \rho(x, x') \ dx \ dx' \tag{1.16}$$

is the transverse beam size, and $\rho(x, x')$ is the normalized distribution function. Therefore, the rms beam size is given by $\sqrt{\beta(s)\epsilon_{rms}}$.

1.2.3 Dispersion

The position of a particle with a momentum deviation Δp with respect to the reference particle with momentum p_0 can be expressed in terms of periodic dispersion function given by

$$x(s) = D(s)\delta \tag{1.17}$$

where $\delta \equiv \Delta p/p_0$ is the fractional momentum deviation. The Hill's equation of motion can be written as [7]

$$x''_\beta + (K_x(s) + \Delta K_x)x_\beta = 0 \tag{1.18}$$

where, to first order

$$\Delta K_x = \left[-\frac{2}{\rho^2} + K(s) \right] \delta \tag{1.19}$$

and $K_x = (1/\rho^2) - K(s)$ and $K(s) = \frac{1}{B\rho}(\partial B_y/\partial x)$. The 2×2 Courant-Snyder matrix can be enlarged to include the dispersion terms as

$$\begin{bmatrix} x \\ x' \\ \delta \end{bmatrix}_2 = \mathcal{M}_C \begin{bmatrix} x \\ x' \\ \delta \end{bmatrix}_1 + \mathcal{M}_C \begin{bmatrix} D(s)\delta \\ D'(s)\delta \\ \delta \end{bmatrix}_1 \tag{1.20}$$

Here, $\mathcal{M}_\mathcal{C}$ is an extended version of Eq. 1.10 with

$$\mathbf{J} = \begin{bmatrix} \alpha & \beta & 0 \\ -\gamma & -\alpha & 0 \\ 0 & 0 & 1 \end{bmatrix} \tag{1.21}$$

1.2.4 Betatron Tune and Chromaticity

An important parameter in colliders is the number of betatron oscillations in one turn which is commonly refered to as *tune* given by

$$Q = \frac{1}{2\pi}\Delta\psi_C = \frac{1}{2\pi}\oint \frac{ds}{\beta} \tag{1.22}$$

The particles with different momenta are focused differently. This effect of momentum dependent focusing is known as chromatic aberration and results in a tune shift given by

$$\Delta Q = \xi\delta \tag{1.23}$$

where the natural chromaticity from quadrupoles is given by

$$\xi = -\frac{1}{4\pi}\oint K\beta ds \tag{1.24}$$

A large chromaticity can result in an overlap of betatron tunes with resonances due to magnet imperfections and lead to beam losses. Furthermore, chromaticity can result in instabilities (head-tail) depending on its sign. Chromaticity correction is usually achieved from non-linear elements like sextupoles. These elements are sources of non-linearities and drive higher order resonances and affect beam stability. They also result in a reduction of the dynamic aperture, the available phase space area sustaining stable motion.

1.2.5 Linear Magnetic Field Errors

The presence of dipole field errors gives an additional transverse orbit displacement. The displacement at a location "s" due to the integrated effect of N deflections θ_i is [23]

$$\Delta x(s) = \frac{\sqrt{\beta}}{2\sin(\pi Q)} \sum_{i=1}^{N} \theta_i \sqrt{\beta_i}\ \cos\big[|\psi(s) - \psi(s_i)| - \pi Q\big]. \tag{1.25}$$

where $\theta_i = \Delta B \Delta s/(B\rho)$ for a dipole, and $\theta_i = (Kl)_i \delta x_i$ for a horizontal displacement of δx_i of a quadrupole. The corresponding change in the length of the closed orbit is given by

$$\Delta L = \sum_{i=1}^{N} \theta_i D(s_i) \tag{1.26}$$

where $D(s)$ is the dispersion function. It can be seen from Eq. 1.25 that dipole perturbations can lead to integer resonances and the closed orbit becomes unstable if the betatron tunes are close to an integer. A large orbit distortion also reduces the available aperture for betatron oscillations.

Similarly, the presence of quadrupole errors results in a perturbation of the β function. The integrated effect on the β function from N quadrupole errors is given by [23]

$$\frac{\Delta\beta}{\beta} = \frac{1}{2\sin(2\pi Q)} \sum_{i=1}^{N} (\Delta Kl)_i \beta(s_i)\ \cos\big[2|\psi(s) - \psi(s_i)| - 2\pi Q\big] \tag{1.27}$$

The corresponding tune shift due to gradient is given by

$$\Delta Q = -\frac{\beta(s_i)}{4\pi} (\Delta Kl)_i \tag{1.28}$$

A second resonance condition at the $\frac{1}{2}$-integer is encountered from quadrupole perturbations which is seen from Eq. 1.27. Therefore, a betatron tune near the $\frac{1}{2}$-integer leads to a diverging solution.

1.3 RHIC Instrumentation

Like most accelerators, RHIC is equipped with a variety of instruments that monitor the beam coordinates, intensities, losses and other beam properties. These instruments not only establish stable circulating beam but also protect the sensitive superconducting elements and electronics crucial for successful operation. Some of the instruments are briefly decribed in the section.

1.3.1 Beam Position Monitors

Beam position monitors (BPMs) are usually stripline or button type monitors used to measure the transverse position of the beam centroid. The transverse beam position is given by

$$x \approx \frac{w}{2}\left[\frac{U_+ - U_-}{U_+ + U_-}\right] \tag{1.29}$$

where $U_\pm$ is either the current or voltage signal from the electrode and $w/2$ is the effective width of the stripline. Fig. 1.5 shows a graphic of a stripline BPM and a cutaway view of a prototype of a RHIC BPM. BPMs are typically

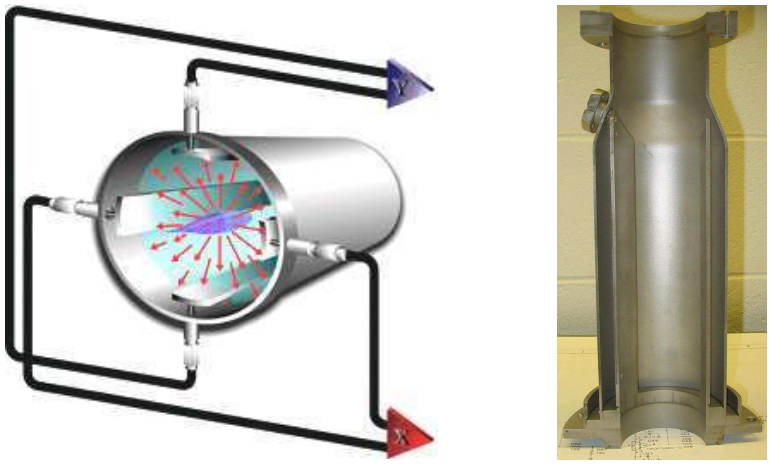

Figure 1.5: Left: A graphic of a stripline beam position monitor [9]. Right: A cutaway view of the RHIC BPM (Courtesy J. Cupolo) designed for cryogenic temperatures.

used to measure the closed orbit averaged over several turns ($\sim 10^4$ or larger). This mode is usually robust and offers a good resolution due to the statistical benefits ($\leq$ 10 μm in RHIC). They are also used to measure turn-by-turn (TBT) beam orbits which contain both position and phase information which is of great interest for the measurement of several linear and non-linear aspects of the lattice. However, issues relating noise, resolution, timing, and fast data acquisition often limit the quality of the data. Part I (chapter 2- 5) of this thesis will focus on bpm reliability, measurement and correction of linear optics and coupling based on TBT data.

1.3.2 Beam Loss Monitors

The beam loss monitors (BLMs) are critical for the protection of the superconducting magnets in RHIC. The RHIC BLMs are ion chambers with an electrode in a cylindrical glass container enclosed in a metal chamber. The chamber is typically filled with dry pressurized gas for sensitivity (Argon in RHIC BLMs). A DC voltage is applied between the outer can and the center electrode to create an electric field. Ionizing radiation passing through the chamber collides with gas molecules producing ion pairs. The primaries and secondaries are swept to the oppositely charged electrode by the electric field. This results in a net current which is then passed through various electronics to amplify and measure the amount beam loss. Pin diodes are also employed in RHIC for fast and sensitive measurement of losses [10].

1.3.3 Profile Monitors

Ionization beam profile monitors (IPM's) measure the beam profile by collecting electrons from background gas ionization [10, 11]. IPM's are primarily used to measure beam emittance and injection matching. RHIC is equipped with four IPM's to measure horizontal and vertical profiles in each ring.

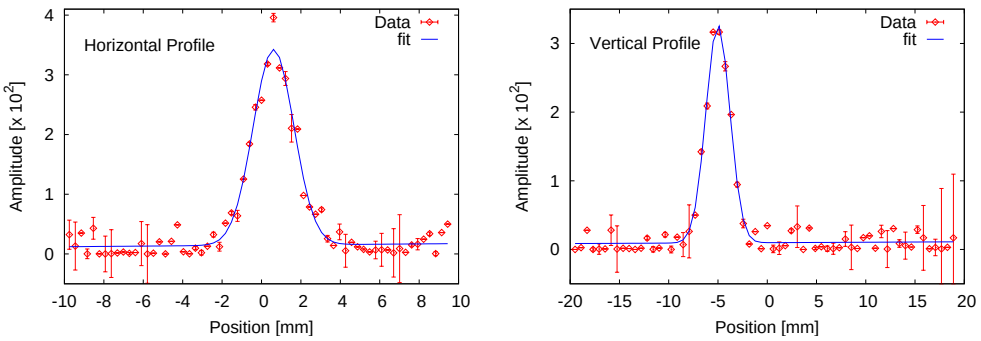

Figure 1.6: A typical plot of the transverse profiles recorded by RHIC IPM's. The data points are averaged over 100 samples. They were taken during Run 2006, p-p collisons at 100 GeV (Fill # 7655). The transverse normalized emittances are estimated to be $\epsilon_x \sim 21\pi$ mm·mrad, $\epsilon_y \sim 15\pi$ mm·mrad.

1.3.4 Wall Current Monitors

A wall current monitor (WCM) is a ceramic break in the beam pipe with several parallel resistors spanning the break [10, 12]. The enclosure is damped

by ferrites to extend the bandwidth from 3kHz out to 6GHz. The voltage induced in the resistors due to image currents of the beam is measured to determine both the beam current and longitudinal profile. RHIC is also equipped with direct current transducers (DCCTs) to measure the average current by balancing primary and secondary currents through a transformer.

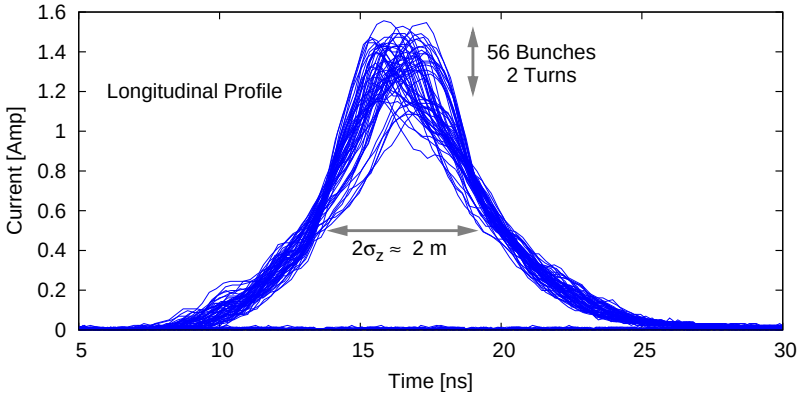

Figure 1.7: A typical longitudinal profile recorded by the RHIC WCM. This data was acquired during Run 2004, p-p collisons with 56 bunches.

1.3.5 Transverse Kickers

RHIC is equipped with fast kicker magnets for injection, beam abort, and tune measurements. Two transverse kicker magnets are available for tune measurements in each ring, capable of generating single turn kick pulses of approximately 140 ns by fast switches [10]. Dedicated dual plane BPMs in each ring are used to measure the beam response (TBT) from a succesion of kicks and calculate tunes which are very useful for machine developement and operation. A typical beam response seen on a BPM due to a transverse kick is shown in Fig. 1.8

1.3.6 AC Dipoles

Unlike a kicker magnet which imparts a impulse kick to the beam, an AC dipole has an oscillating field to induce coherent large amplitude oscillations in the beam when driven close to a resonance. The amplitude of the oscillations is given by [13]

$$x(s) \approx \frac{1}{4\pi|\delta Q|}\frac{B_d l}{B\rho}\sqrt{\beta(s)\beta_d} \tag{1.30}$$

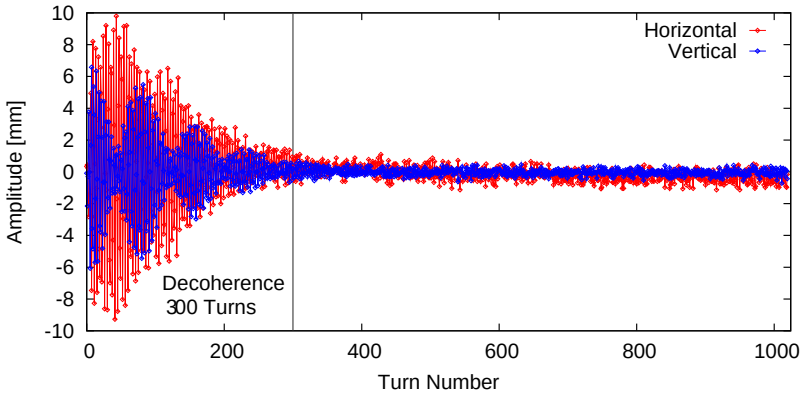

Figure 1.8: Typical beam response as seen on a BPM due to transverse kick in both planes. The decoherence time is in this case is approximately 300 turns which is mainly dominated by linear chromaticity and also some non-linear de-tuning.

where d is the location of the AC dipole, and $\delta Q = Q_0 - Q_d$ is the tune separation between the drive frequency and the betatron frequency. An AC dipole can be ramped adiabatically and has the advantage of preserving the beam emittance unlike an impulse kick. Coherent betatron oscillations overcome the

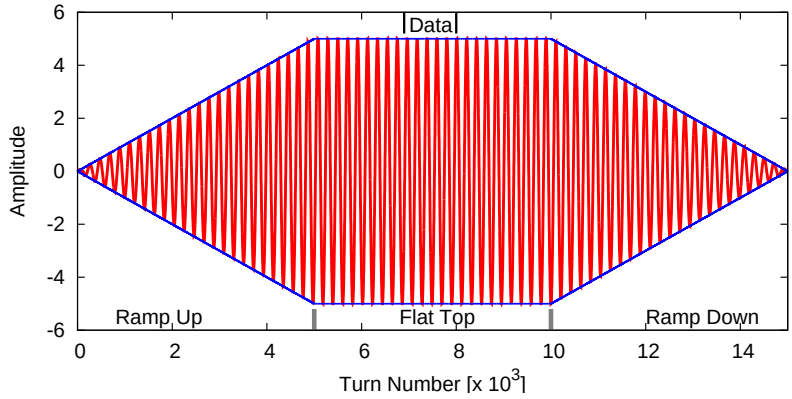

Figure 1.9: Graphic of the ramp up, flat top, and ramp down of an AC dipole field.

difficulties associated with decohered oscillations to measure beam properties with known numerical techniques (for example broadening of the Fourier spectrum). In principle, the length of the AC dipole excitation is limited by the data acquisition capability. In Part I of this thesis, AC dipole data is exten-

sively used to measure linear optics and coupling. Several other uses like accelerating through depolarizing resonances [15] and non-linear studies [16, 17] make the AC dipole an unique and invaluable device.

Table 1.2: RHIC parameters for Au-Au, p-p, and Cu-Cu during Runs IV and V. Tune scan simulations and experiments found betatron tunes at $Q_x = 28.72$, $Q_y = 29.73$ to provide better dynamic aperture and fewer spin resonances for polarized protons [20].

			Gold	**Protons**	**Copper**
parameter	symbol	unit	value	value	value
Mass number	A	-	197	1	63
Atomic number	Z	-	79	1	29
Number of ions/bunch	N_b	10^9	1	100	4.5
Number of bunches/ring	-	-	*variable, from 28 to 110*		
Circumference	C	m	3833.85		
Energy per beam injection	E	GeV/n	10.8	28.3	12.6
Energy per beam store	E	GeV/n	100	100 & 190	100
Transition energy	γ_t	-	22.89		
Magnetic rigidity injection	$B\rho$	T m	81.1	81.1	81.1
Magnetic rigidity store	$B\rho$	T m	839.5	339.5	724.6
Dipole field injection	B	T	??	0.33	???
Dipole field store	B	T	??	1.37	???
Betatron tune horizontal	Q_x	-	28.23		29.72
Betatron tune vertical	Q_y	-	28.22		29.73
β^* at IP injection	β^*	m	10		
β^* at IP store	β^*	m	1-3		
Quadrupole gradient	-	T/m	≈71		
Operating temp, ^{4}He	T	K	4		
Harmonic number injection	h	-	360	360	360
Harmonic number store	h	-	2520	360	2520
RF voltage injection	V	MV	0.3	0.1	0.3
RF voltage store	V	MV	2-4	0.3	2-4
RF frequency injection	$\omega_{\rm rf}$	MHz	28.15	28.15	28.15
RF frequency store	$\omega_{\rm rf}$	MHz	198	28.15	198
Synchrotron freq. injection	Q_s	Hz	120	25	145
Synchrotron freq. store	Q_s	Hz	333	43	270
Energy spread injection	$\Delta E/E$	10^{-3}	±1.49	±1.26	??
Energy spread store	$\Delta E/E$	10^{-3}	±1.49	±0	??
Bunch area injection	$S_{95\%}$	eV s/u	0.5	0.5	0.7
Bunch area store	$S_{95\%}$	eV s/u	1.1	1.2	1.0
Normalized emittance	ϵ_n	mm mrad	10π	20π	10π